

Fire Radiative Power products (Giglio et al. 2016). Here, we use consistent reprocessing with input from MODIS Collection 6 for the entire period of 2003–22. The 14% bias with respect to Collection 5 has been corrected, and the satellite- and observation time-specific bias correction factors from Hüser et al. (2018) have been applied in order to compensate for several outages of observations from the MODIS instruments during 2022. The *Aqua* and *Terra* satellites carrying MODIS have been in drifting orbits during 2022 with an overall shift of the local equator crossing times of <15 minutes (<https://aqua.nasa.gov/sites/default/files/AquaStatus.pdf>; <https://terra.nasa.gov/wp-content/uploads/2022/09/Orbit-Changes-Terra.pdf>); we consider this to be negligible for GFAS. The time series in Plate 1.1 also puts GFAS in the context of GFED4s, which is mostly based on burnt area observation and dates back to 1997 (van der Werf et al. 2017).

4. PHENOLOGY OF PRIMARY PRODUCERS

—D. L. Hemming, O. Anneville, Y. Aono, T. Crimmins, N. Estrella, A. Menzel, I. Mrekaj, J. O’Keefe, T. Park, A. D. Richardson, J. Rozkošný, T. Rutishauser, T. H. Sparks, S. J. Thackeray, A. J. H. van Vliet, and F. West.

During 2022, land surface phenology derived from the MODIS Normalized Difference Vegetation Index (NDVI, a dimensionless index of the difference between visible and near-infrared reflectance of vegetation cover, where higher values indicate denser, green vegetation) over the Northern Hemisphere (>30°N; Park et al. 2016), was compared to NDVI over the 2000–20 baseline period (Fig. 2.78). The hemispheric mean Start and End of Season (SOS_M and EOS_M) for the

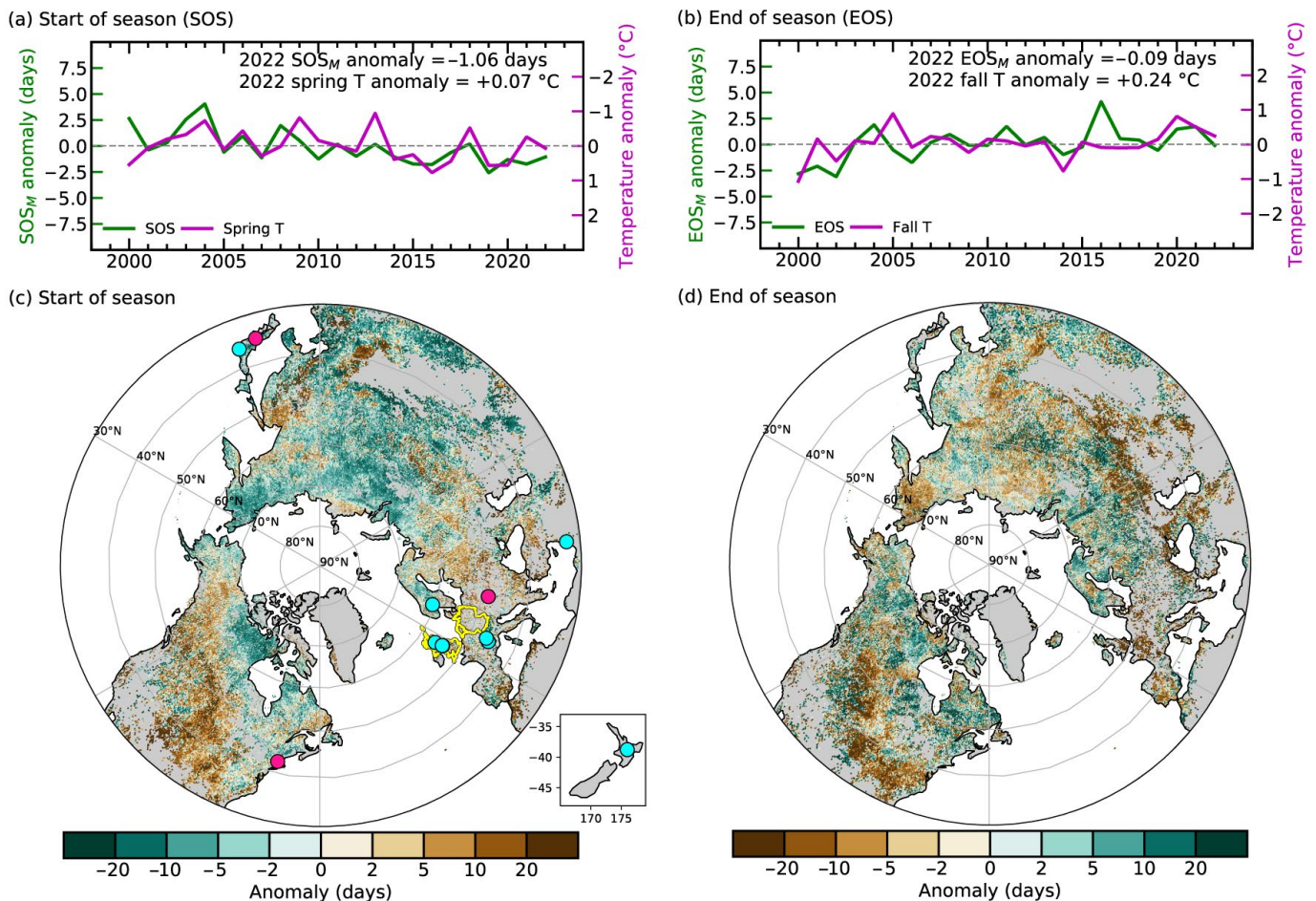


Fig. 2.78. (a) Time series of area-mean anomalies (days relative to 2000–20 baseline) in MODIS Normalized Difference Vegetation Index (NDVI)-based vegetation-growing-season onset (start of season, SOS_M , green) and satellite-derived (MERRA-2) spring (Mar–May, pink) temperature for the Northern Hemisphere. (b) Same as (a) but for growing season end (end of season, EOS_M , green) and autumn (Sep–Nov, pink) temperature. Note the temperature scale reversal for (a). (c),(d) Spatial pattern of (c) SOS_M and (d) EOS_M anomalies in 2022 with respect to the baseline. Highlights identify the location of sites shown in Figs. 2.79 and 2.80 and discussed in the text (country mean phenology data, yellow; site PhenoCam and phenology observations, magenta; lake phytoplankton, blue).

baseline period is 16 May and 11 October, respectively, and in 2022, SOS_M was 1.1 days earlier and EOS_M was similar to the baseline (Figs. 2.78a,b; Table 2.11). Regionally, earlier SOS_M occurred across central and northeastern Eurasia (EA), Alaska, and northern Canada. The warmer spring ($+0.23^\circ\text{C}$) led to 2.5 days earlier SOS_M in EA. Most of North America (NA) experienced later SOS_M ($+1.7$ days) in 2022 (Fig. 2.78c) due to the colder (-0.18°C) and wetter ($+0.05$ mm day $^{-1}$) spring, particularly over U.S. croplands. Northern NA and western EA showed later EOS_M ($+0.8$ days) whereas earlier EOS_M (-0.4 days) was observed in southern NA and eastern EA (Fig. 2.78d). Time series of the two decades of the MODIS record show continuous advancement and delay trends in SOS_M and EOS_M (SOS_M : -1.6 ± 0.4 days decade $^{-1}$, $p < 0.001$; EOS_M : $+1.2 \pm 0.5$ days decade $^{-1}$, $p = 0.07$).

PhenoCam data (Seyednasrollah et al. 2019) helped link the coarse resolution of satellite-derived phenology with fine-resolution visual observations on organisms and ecosystems (Richardson 2019). PhenoCam estimates (2008–22) of SOS (SOS_{PC}) and EOS (EOS_{PC}) at Harvard Forest, a deciduous forest in Massachusetts (United States) were compared with ground observations of red oak (*Quercus rubra*; SOS_{RO} and EOS_{RO} ; Richardson and O’Keefe 2009; O’Keefe

Table 2.11. Start of season (SOS), end of season (EOS), and full bloom dates (FBD; for native cherry tree observations only) for MODIS mean across the Northern Hemisphere (NH MODIS, $>30^\circ\text{N}$), land phenology records in USA (Harvard: PhenoCam, red oak, and MODIS mean across Harvard Forest; USA National Phenology Network, USA-NPN, mean covering northeastern United States), Europe oak records (Germany, Netherlands, Slovakia, UK, and MODIS mean across UK) and Japan (native cherry tree observations and MODIS mean across Japan). The baseline period is 2000–20 for all records except PhenoCam and NPN, which have baseline periods of 2008–22 and 2011–22, respectively, spanning the available observations. Negative/positive values represent earlier/later dates.

Location/Record	SOS/FBD 2022 (date)	SOS/FBD Baseline (date)	SOS/FBD Difference 2022-Baseline (days)	EOS 2022 (date)	EOS Baseline (date)	EOS Difference 2022-Baseline (days)
NH MODIS	15 May	16 May	-1	11 Oct	11 Oct	0
Harvard MODIS	26 Apr	24 Apr	-2	1 Dec	5 Dec	+3
Harvard PhenoCam	9 May	7 May	-2	16 Oct	22 Oct	+5
Harvard red oak	13 May	6 May	-7	18 Oct	19 Oct	0
USA-NPN	7 May	6 May	-1	27 Sep	3 Oct	+6
UK MODIS	6 Apr	30 Mar	-7	23 Dec	12 Dec	-10
Germany	29 Apr	28 Apr	+1	12 Nov	6 Nov	+6
Netherlands	17 Apr	20 Apr	-3	19 Dec	27 Nov	+22
Slovakia	1 May	26 Apr	+6	14 Oct	18 Oct	-4
UK	19 Apr	24 Apr	-5	10 Dec	1 Dec	+9
Japan MODIS	9 Apr	21 Apr	-12	-	-	-
Japan	1 Apr	6 Apr	-5	-	-	-

2021) and MODIS (SOS_M and EOS_M) for the associated pixel (Figs. 2.79a,b). These were also compared with red oak observations contributed to *Nature's Notebook*, the United States National Phenology Network's (NPN) monitoring across the northeastern United States (Rosemartin et al. 2014; Crimmins et al. 2022). In 2022, SOS_{PC} , SOS_{RO} , and SOS_M were zero, three, and two days later, respectively, compared to 2021. EOS_{PC} , EOS_{RO} , and EOS_M were 17, 7, and 13 days earlier compared to 2021 (Figs. 2.79a,b). Interannual variability of start and end of season for Harvard Forest are broadly consistent with those from the NPN, which underscore the value of volunteer-contributed data for tracking phenology at local to continental scales. The earlier EOS_{PC} in 2022 yielded a growing season of 160 days, more than two weeks shorter compared to 2021 and a full week shorter compared to the 2011–20 average (167 ± 7 days; Table 2.11).

'First leaf'/'start of leaf unfolding' (SOS_0) and 'leaf falling'/'bare tree' (EOS_0) dates for oak (*Quercus robur* and/or *Q. petraea*) from Germany (D), the United Kingdom (UK), Netherlands (NL), and Slovakia (SK) are presented (Figs. 2.79c,d). In 2022, SOS_0 dates varied across Europe from 5 and 3 days earlier than the baseline (in UK and NL) to 1 and 6 days later (in D and SK), while EOS_0 dates were earlier by 4 days (SK) and later by 6, 9, and 22 days (D, UK, and NL; Table 2.11).

Start- and end-of-season events across Europe are strongly influenced by temperature (Menzel et al. 2020); SOS_0 advances by four to six days per 1°C increase in the mean February–April temperature, and EOS_0 is delayed by two to four days per 1°C increase in the mean September–October temperature. In 2022, the later EOS_0 dates in D, UK, and NL were, in part, associated with unusually high autumn temperatures, encouraging leaf activity and resulting in a longer 2022 'oak season' at these locations (for UK, see Kendon et al. 2022). In SK, high spring, summer, and autumn air temperatures and soil moisture deficits in 2022 encouraged later leaf out and early leaf fall and led to the shortest oak season since 2000.

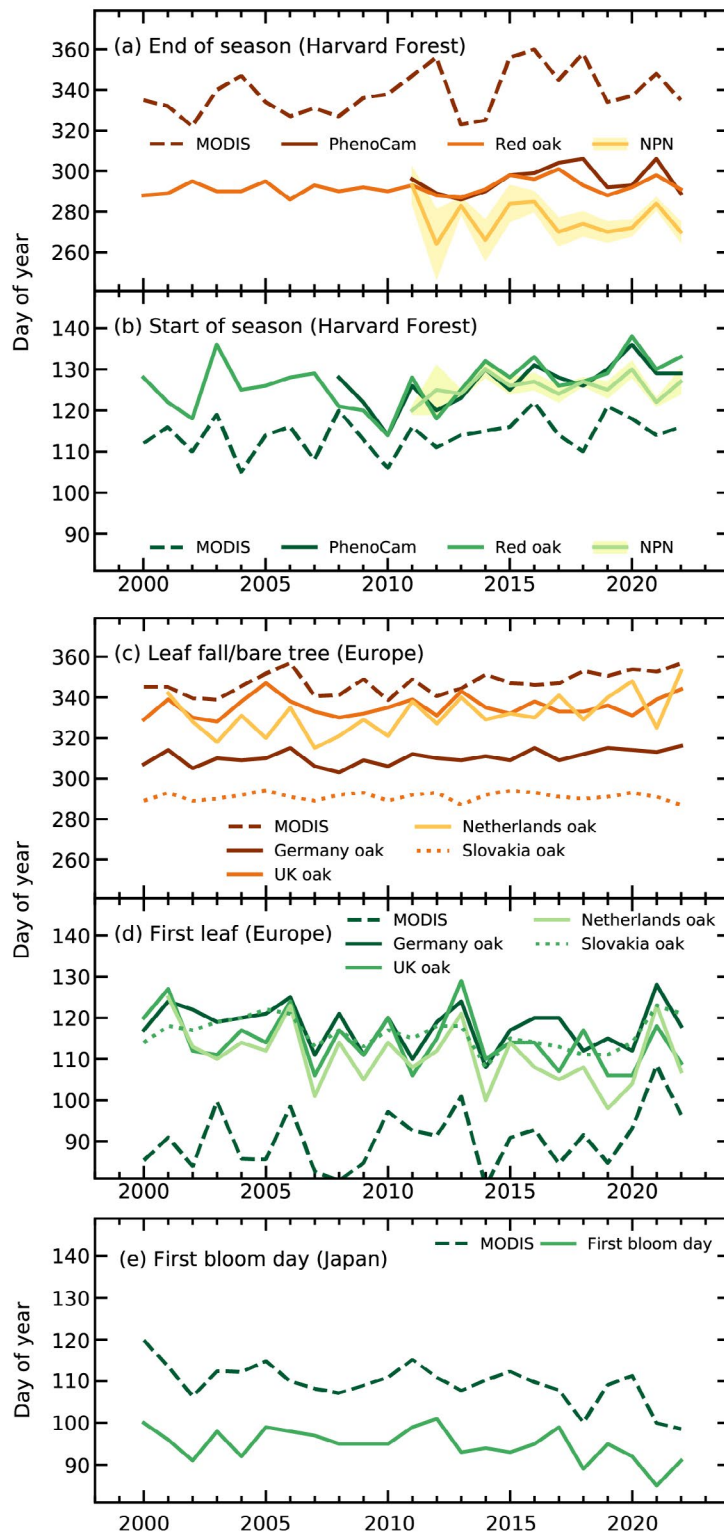


Fig. 2.79. Day of year of spring (green shades) and autumn (orange and brown) vegetation phenology indicators for (a),(b) Harvard Forest, Massachusetts, derived from PhenoCam, red oak ground observations, MODIS remote sensing (dashed), and USA-National Phenology Network (NPN) regional-scale means for red oak (calculated across the northeastern states of Pennsylvania, New Jersey, New York, Connecticut, Rhode Island, Massachusetts, Vermont, New Hampshire, and Maine, ± 1 std. error shaded), (c),(d), Germany, UK, Netherlands, and Slovakia mean oak and MODIS Europe mean, and (e) Kyoto, Japan, full bloom day observations for cherry trees and MODIS Japan mean start of season.

In Kyoto, Japan, full bloom dates (FBD) for a native cherry tree species, *Prunus jamasakura*, were acquired from historical documents dating back to 812 AD (Aono and Kazui 2008) and updated with current observations at Arashiyama, which are compiled from daily observations made by railway passengers at train stations and recorded in newspapers and on web sites (Fig. 2.79e). In 2022, FBD was five days earlier than the 2000–20 mean (Table. 2.11).

Monitoring data on lake water concentrations of the photosynthetic pigment chlorophyll-*a* were available to estimate spring phytoplankton phenology in 1 Southern Hemisphere and 10 Northern Hemisphere lakes (Fig. 2.80). Seasonal timing was quantified for start of season (SOS_L ; Park et al. 2016), day of maximum concentration (DOM_L), and center of gravity (COG_L , an estimate of the mid-point of the plankton bloom; Edwards and Richardson 2004). Lake basins showed great interannual variation and mixed phenological behavior in 2022 relative to the 2000–20 baseline. The Norway lake, Mjøsa, and the Southern Hemisphere lake in New Zealand, Taupo, showed different seasonal changes to other lakes related to snow melt and southern season, respectively. SOS_L occurred earlier than the baseline median for most (8 of 11) lakes, and DOM_L occurred later in most lakes (8 of 11). For COG_L , no consistent pattern was observed.

5. VEGETATION OPTICAL DEPTH

—R. M. Zotta, R. van der Schalie,
W. Preimesberger, L. Moesinger,
R. A. M. de Jeu, and W. Dorigo

Microwave radiation emitted or reflected by Earth's surface is strongly affected by available surface water, including that which is stored in living biomass. The portion of the radiance attenuated by the canopy is expressed by vegetation optical depth (VOD), a parameter used in radiative transfer models to describe radiance interaction with vegetation. VOD is closely related to canopy water content (Konings et al. 2017), leaf area index (Vreugdenhil et al. 2017), and gross primary production (Teubner et al. 2019; Wild et al. 2022) and is a good indicator of vegetation response to climate variability. Positive

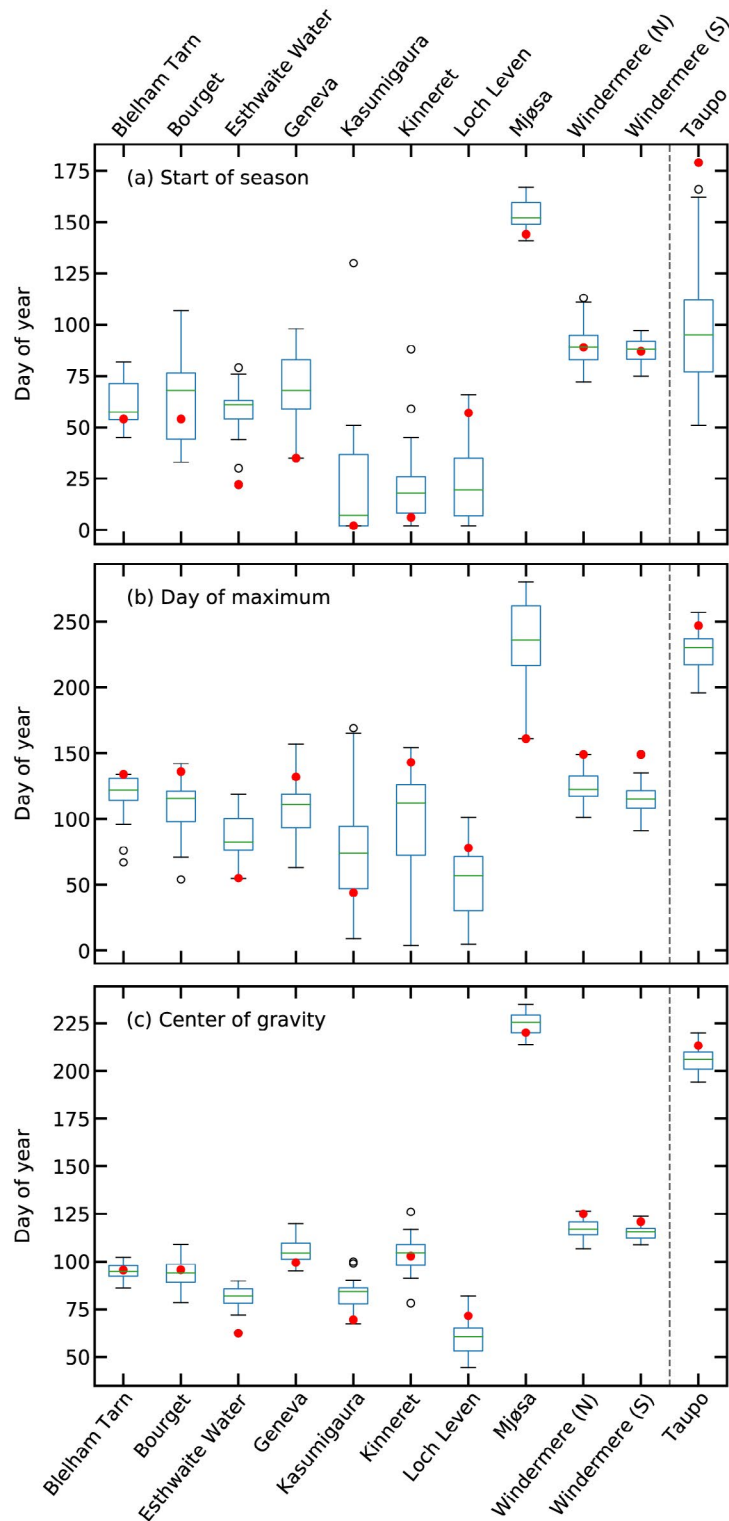


Fig. 2.80. Phenological metrics based on lake chlorophyll-*a* concentrations, as a proxy of phytoplankton biomass: (a) start of season, (b) day of maximum, and (c) center of gravity. Boxplots show variation during the 2000–20 baseline period, and red dots show 2022 values. Dashed line identifies Northern Hemisphere (Blelham Tarn in UK, Bourget in France, Esthwaite Water in UK, Geneva in France/Switzerland, Kasumigaura in Japan, Kinneret in Israel, Loch Leven in UK, Mjøsa in Norway, north and south basins of Windermere in UK) and Southern Hemisphere (Taupo in New Zealand) lakes.